The 8th European Congress on Computational Methods in Applied Sciences and Engineering
ECCOMAS Congress 2022
5-–9 June 2022, Oslo, Norway

# A NUMERICAL SET-UP FOR THE SIMULATION OF INFECTION PROBABILITY FROM SARS- COV-2 IN PUBLIC TRANSPORT VEHICLES

**Eugenio Schillaci[1,*], Jordi Vera[1], Nina Morozova[1] and Joaquim Rigola[1]**

[1] Universitat Politècnica de Catalunya - Barcelona Tech (UPC),
ESEIAAT, C/ Colom, 11, 08222, Terrassa (Barcelona), Spain
www.cttc.upc.edu

[*] corresponding author: eugenio.schillaci@upc.edu

**Key words:** RANS simulation, CFD integrated Wells-Riley Model, public transport infection, SARS-CoV-2

**Abstract.** In this work, a numerical framework aimed at simulating the transport of contaminants and infectious agents within a closed domain is presented. The method employs mature CFD algorithms to calculate air fields with reasonable computational costs. The main objective is to give fast response to stakeholders about air quality indicators in the design phase of HVAC systems. A discussion regarding the size and characteristics of different contaminants is proposed, highlighting the most appropriate methods and coefficients needed to simulate their transport. Next, the methodology employed to evaluate the risk of infection is presented. The numerical set-up, based on the *buoyantBoussinesqPimpleFoam* solver in OpenFOAM, was tuned by simulating the well-known case of the heated floor cavity, providing accurate results. Hence, the case study of a transport vehicle of generic shape is presented, in order to show possible results in terms of air-age distribution, PM2.5 distribution, and global infection risk matrix.

## 1 INTRODUCTION

The outbreak of SARS-CoV-2 has shown the importance of indoor air quality control and flow pattern studies. In this sense, Computational Fluid Dynamics (CFD) simulations have always been a powerful tool to study air movement and contaminant transport. In the case of HVAC installations, CFD can help understand the flow patterns and propose new alternatives to improve the air quality, which can result in a reduction of new infections. The numerical method is built on the basis of the turbulent fluid solver *buoyantBoussinesqPimpleFoam*, present on the open-source platform OpenFOAM. The solver integrates the transport of a scalar quantity called air-age used to measure indoor air quality. In the simulations, the $k-\varepsilon$ RANS turbulence model previously tested in [1] is employed, and an original methodology is introduced to determine susceptibility to infection by airborne transmission of the virus. This is done by running multiple simulations of the contaminant transport for a stationary flow, placing the main source of contaminant in a different location and studying its effect on the rest of the users of the vehicle. A convection-diffusion equation with variable source term is employed to model contaminant transport [2, 3]. Realistic parameters for the contaminant generation and inhalation rate, as

well as for its diffusion in the air, are employed [4]. Once the contaminant concentration distribution is resolved, an integration over time is performed to obtain the probability of infection in each susceptible location using the CFD integrated form of the Wells-Riley model [2, 3]. This numerical method allows the study of air quality and the diffusion of contaminants in means of transport (or other closed places) in which air conditioning and/or purification systems are active. The simulations allow to choose the operating parameters (positions of the vents, air velocity, recirculation rate, positioning of the seats) that minimize the risk of infection for the users of the service.

## 2 NUMERICAL SET-UP

### 2.1 CFD Model

The numerical method proposed in this work resolves Navier-Stokes equations on 3D unstructured domains. An unsteady RANS solver is ran to get statistically steady-state solution for velocity, $\bar{\mathbf{v}}$ and pressure, $\bar{p}$, within the domain of a public transport vehicle. The main governing equation for momentum conservation is the following, taking into account a linear eddy viscosity model approximation:

$$\frac{\partial \rho \bar{\mathbf{v}}}{\partial t} + \nabla \cdot (\rho \bar{\mathbf{v}} \cdot \bar{\mathbf{v}}) = \mathbf{g} - \nabla \bar{p'} + \nabla \cdot (\mu_{\text{eff}} \nabla \bar{\mathbf{v}}) + \nabla \cdot \left[ \mu_{\text{eff}} \, \text{dev2} \left( \nabla \bar{\mathbf{v}} \right)^T \right] \tag{1}$$

where $\mu_{\text{eff}}$ is the effective dynamic eddy viscosity, evaluated as $\mu_{\text{eff}} = \mu + \mu_t$. The $dev2$ operator is defined as follows:

$$\text{dev2} \left( \phi \right) = \phi - \frac{2}{3} \text{tr} \left( \phi \right) I \tag{2}$$

The incompressibility constraint is introduced during resolution to account for mass conservation. Simulations were run on the OpenFOAM software. In particular, the *pimpleFoam* solver was employed, which is a transient solver for turbulent flow in incompressible fluids. The $k - \varepsilon$ turbulence model [5] is employed, while the $epsilonWallFunction$ boundary condition is used to provide a wall constraint on the turbulent kinetic energy dissipation rate. In this approach, a two transport-equation linear-eddy-viscosity turbulence closure model is employed, thus, solving two additional transport properties, namely, turbulent kinetic energy, $k$, and turbulent kinetic energy dissipation rate, $\varepsilon$, for the calculation of $\mu_t$, defined as

$$\mu_t = C_\mu \frac{k^2}{\rho \epsilon} \tag{3}$$

The transport of air-age, $\tau$, was added to the solver, representing a reliable indicator to analyse the air quality within a closed environment

$$\frac{\partial \tau}{\partial t} + \nabla \cdot (\bar{\mathbf{v}} \tau) - \nabla \cdot \left( \frac{\nu_{eff}}{\sigma_\tau} \nabla \tau \right) = 1 \tag{4}$$

where $\nu_{eff} = \nu + \nu_t$ is the effective kinematic viscosity, sum of the molecular kinematic viscosity, which is an intrinsic property of the fluid, and the turbulent kinematic viscosity, which characterizes the turbulence of the flow. $\sigma_\tau$ is the equivalent Prandtl number for $\tau$ and represents the ratio between the diffusion coefficients of the linear momentum and the air age.

### 2.2 Contaminant transport

Additionally to Navier-Stokes and air-age equations, the transport of additional quantities is performed in this work, aimed at studying the distribution of viruses or other contaminants within the environment. The transport of a quantity $\phi$, e.g. in terms of volumetric concentration, whose particles are sufficiently small in size, can be studied by a typical convection-diffusion equation with a source term:

$$\frac{\partial \phi}{\partial t} + \nabla \cdot (\phi \mathbf{v} - \alpha_\phi \nabla \phi) = S_\phi \tag{5}$$

where $S_\phi$ is the source term, only considered if a source term for $\phi$ is present within the domain. Before defining the concept of *sufficiently small in size*, we need to mention the fact that the issue of the transport of contaminants will be analyzed in this work under two different paradigms. On the one hand, there is the issue of the transport of infectious elements, such as the viruses responsible for the SARS-CoV-19 disease. In this case the problem of quantifying the infection probability arises, as a function of the amount of infectious agent in the air. On the other hand, a more general problem arises related to the quality of the air breathed by the users of the transport vehicle. In this case, the aim is to measure the internal levels of contamination of some markers, and compare them with reference levels identified as acceptable by the health authorities. The size of viruses is generally very small, for example, the virus responsible for SARS-CoV-19 has an estimated size of between 50 and 150 nm. Therefore, a study through Eq. 5 is highly realistic. The quantification of viruses and bacteria can be done by introducing the concept of quanta concentration $\phi$ [quanta/m$^3$] which gets transported over a fluid field (as discussed in detail in the Sec. 4). A separate discourse must be made for generic air pollutants, present in a more or less industrial urban environment and therefore also present within public transport vehicles. Common contaminants, along with their size and characteristics, are listed in the following table:

Table 1: Possible pollutants to be analyzed in Air Quality CFD studies.

| | Size | Remarks |
|---|---|---|
| $CO_2$<br>$NO_x$ | Very small size (molecular level) | - Easy to perform on-time measurements<br>- Not effective to assess filtering strategies |
| PM10<br>PM2.5 | $\leq$10 µm<br>$\leq$2.5 µm | - Easy to perform on-time measurements<br>- Removed by common filters |
| Bacteria<br>Fungi | 0,5 µm - 5 µm<br>2 µm – 50 µm | - Difficult and slow to analyze experimentally |

In general, the method of studying the transport of contaminating particles can be established through the Stokes number, Stk, a dimensionless number characterizing the behavior of particles suspended in a fluid flow:

$$\text{Stk} = \frac{t_0 v_0}{l_0} \tag{6}$$

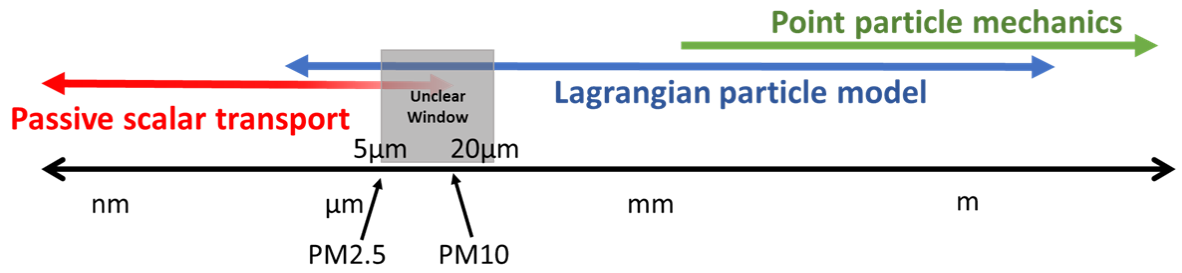


Figure 1: Classification of modelization approach versus particle size.

where $t_0$ is the relaxation time of the particle (the time constant in the exponential decay of the particle velocity due to drag), $v_0$ is the fluid velocity of the flow well away from the obstacle and $l_0$ is the characteristic dimension of the obstacle (typically its diameter). A particle with a low Stk number follows fluid streamlines (perfect advection), while a particle with a large Stk is dominated by its inertia and continues along its initial trajectory. For mild Stk numbers, e.g. Stk $\simeq 1$, both fluid and particle effect should be taken into account. For low Stk numbers, a passive scalar model can be applied, the particle follows the movement of the fluid and its distribution is evaluated as a concentration scalar parameter described by a convection-diffusion equation. As Stk increases, Eulerian-Lagrangian models must be employed, and a finite number of particles is simulated. Each particle is solved using Newton equations and the movement is coupled with the velocity field solution of the Navier-stokes equations. For an important number of particles, this approach is more complex and computationally expensive. Certain debate exists regarding the particle size and the Stokes number for which it may be considered appropriate to use an Eulerian transport model: Liu et al. [6] considers 20 $\mu m$ as superior limit, while Hathway et al. [7] study the transport of contaminats with $d = 2.5$ $\mu m$ as median parameter. A general overview is proposed by Isukapalli et al. [8], and resumed graphically in Fig. 1. Resuming, it has been chosen to employ PM2.5 as representative parameter the measure air quality. Indeed, it seems reasonable to consider the transport of these particles by means of a convection-diffusion transport equation.

**Diffusion coefficients:** To determine the diffusion coefficient $\alpha_\phi$ of Eq. 5 different approaches can be adopted. In general, $\alpha_\phi = (\alpha + \alpha_t)$, sum of molecular and turbulent diffusivity. If the molecular diffusivity is well known, as in the case of popular species and contaminants, it can be directly set, while $\alpha_t$ is calculated by the turbulent solver. In other cases, the formula from [9] for the calculation of $\alpha_\phi$ can be employed:

$$\alpha_\phi = 0.824 \cdot \frac{Q}{\sqrt[3]{VN^2}} \tag{7}$$

where $Q[\mathrm{m}^3/\mathrm{s}]$ is the total volumetric flow, $V[\mathrm{m}^3]$ is the room volume, and $N[\mathrm{m}^3/s]$ is the number of air supply vents. The equation considers that the effects of the turbulence on the diffusion due to mixing is much more important than the molecular diffusion. Introducing this constant $\alpha_\phi$ model for all the domain will probably not be as accurate as using a turbulent model

for this property with its specific value for each region, but it will probably be good enough when considering that other factors (for example, moving people) are not taken into account.

**Source term:** As already commented, the source term $S_\phi$, is considered only if an infection source is present within the domain. For the case of virus transport, the value of the source term $S_\phi$ is related to the quanta generation rate concept explained in Sec. 4, and is introduced within the domain to take into account the presence of an infected subject. The methodology, as well as the empirical coefficients employed to calculate the infection probability for the specific case of SARS-CoV-2 are detailed in Sec. 4. On the other side, when considering PM transport, no sources are present within the domain, as the source of contamination comes from the external air.

## 3 NUMERICAL METHOD VALIDATION

The ventilated and heated rectangular cavity proposed by Nielsen [10] is used as a test case to validate a numerical set-up which will be employed to perform thermo-ventilation studies. The domain consists of a rectangular cavity reported in Fig. 2a. Fresh air is supplied to the cavity from a thin inlet slot of height $h = 0.056H$ located at the top-left side. The air leaves the cavity through a thin slot of height $t = 0.16H$ located at the bottom-right side (plane $x = L$). The air is introduced horizontally at a velocity $U_0 = 15.2m/s$. ($Re = 7100$) with a turbulence intensity of the order of 5% and a temperature $T = 295.15K$. All the walls of the cavity are considered adiabatic except for the floor where a uniform heat flux density is imposed ($q = 563W/m^2$ or $Q = 128W$). In order to introduce the natural convection effect due to the heated floor, a variant of the *pimpleFoam* solver is employed here, i.e. the *buoyantBoussinesqPimpleFoam* solver. This solver still employs an incompressible flow formulation, i.e. the density is constant in all the terms, except in the calculation of the gravity force, where the density is considered variable to take into account buoyant effects (Boussinesq approximation). In particular, the gravity force is calculated as

$$f_b = -\rho\beta(T - T_0)\mathbf{g} \tag{8}$$

where $\beta$ is the air expansion coefficient and $T_0$ is the reference temperature. This enables natural convection problems to be dealt without having to solve for the complete compressible formulation with Navier–Stokes equations. This solver also solves energy conservation to obtain the temperature evolution needed to evaluate the buoyancy effect. The thermo-physical coefficients used in the simulations are constant and must be chosen to represent fairly well the behavior of the flow in the range of temperatures expected in the simulation. The adoption of a similar set-up for air quality studies has been done lately by several authors, e.g Limane et al. [11]. Different velocity and temperature profiles are available in the literature to perform the set-up validation [10, 11]. In Fig. 2 results for the horizontal velocity profile along $z$, temperature profile along $x$ at $y = 0.67W, z = 0.25H$ and temperature profile along $x$ at $y = 0.67W, z = 0.0$ are proposed. Numerical results were obtained on a Cartesian mesh of $381 \times 127$ cells, employing a 2D approximation of the domain. Even so, the the velocity profile is reproduced with good accuracy, while only small errors are obtained on temperature profiles.

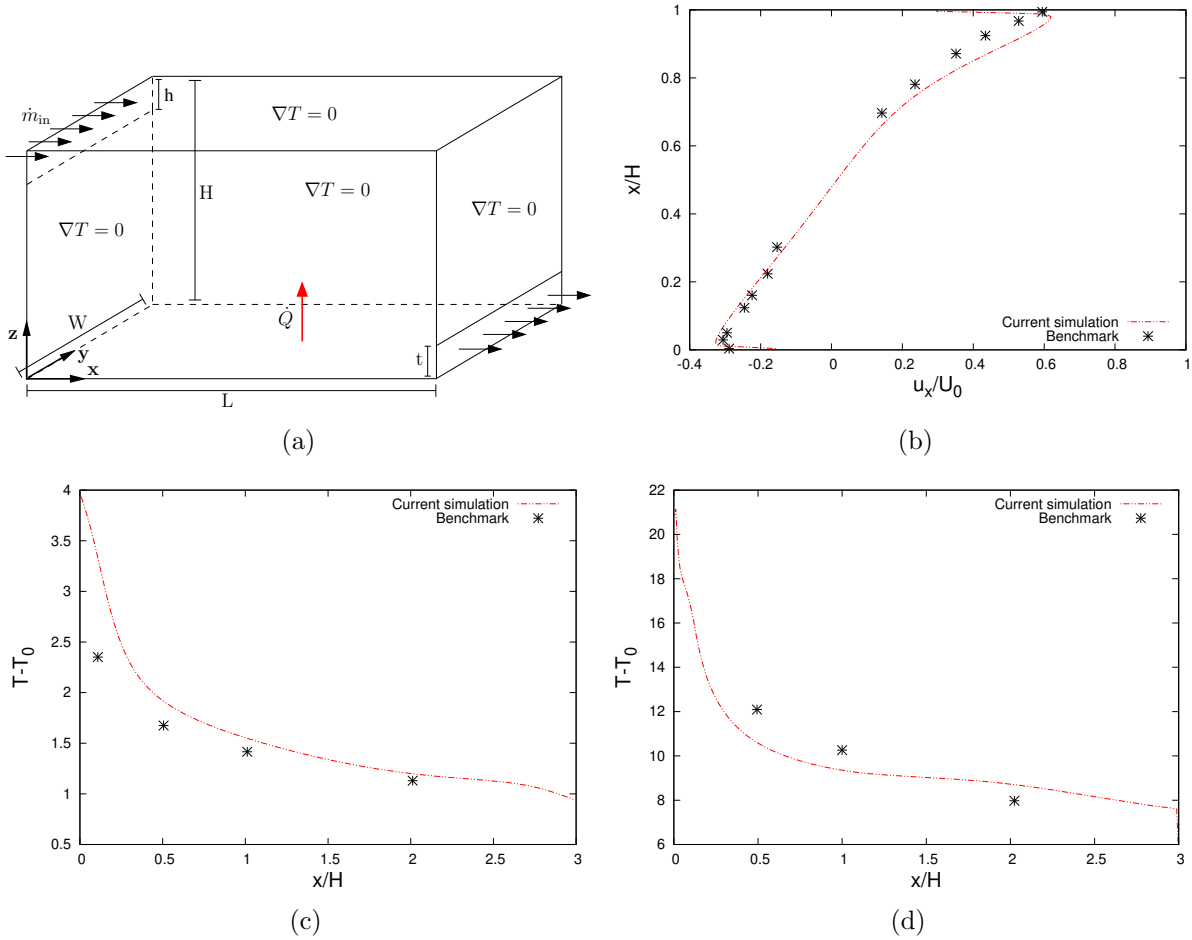


Figure 2: Heated floor cavity validation case: (a) validation case domain; (b) horizontal velocity profile along $z$; (c) temperature profile 1 along $x$ at $y = 0.67W, z = 0.25H$; (d) temperature profile 2 along $x$ at $y = 0.67W, z = 0.0$.

## 4 INFECTION RISK METHODOLOGY

### 4.1 Wells-Riley Model

According to the Wells-Riley model, the probability of infection follows a Poisson distribution, being $q$ the quanta breathed by a person over a certain period of time

$$P = 1 - e^{-q} \tag{9}$$

where $q$ is a quantum of infection or *quanta* [12, 2], representing the number of infectious airborne particles required to infect a person based on a Poisson distribution. The probability of being infected by a single quanta is 63.2%. To clarify, if you breathe a certain quantity of air over a period of time, and this volume of air had an equivalent of a quanta in terms of infectious

particles, you have 63.2% chances of getting infected. In terms of quanta generation and absorption, every disease is different. However, the expulsion rate of virus particles from infected subjects, the quantity inhaled from susceptible people, and the probability of being infected as a function of exposure time can be determined as a result of empirical studies. In this work, we employed empirical data from different sources to estimate the quanta generation rate [14, 4]. It must be noticed, that there is some variation between sources due to the high uncertainty which characterize this kind of empirical magnitudes. However, the results are capable of giving an order of magnitude for the probability of infection and to compare the contaminants removal effectiveness between different configurations. For our cases we will consider the quanta generation rate (quanta emitted or exhaled by one person) reported in Tab. 2, corresponding to the source term for the virus transport equation.

Table 2: Quanta generation rate for COVID-19 in our simulations. $f_a$ is the mask correction factor

| **Case** | $S_\theta$ | **Assumption** |
|---|---|---|
| Person breathing | $25 \cdot f_a$ | Average behavior (some seated, some standing, some talking) |
| Person coughing | $200 \cdot f_a$ | Person singing or loudly speaking |

In our studies, the concentration of quanta over time $\phi(t)$ in the proximity of a each susceptible subject is tracked. Then, considering the volumetric flow of air that a person breathes, we can calculate the quantity of $\phi$ inhaled ($\mathcal{I}_\phi$). A person breathing rate [13] is 7.5 $l/min$ when resting, and up to 120 $l/min$ in heavy exercise. We will consider the people of the bus to be in a resting mode, so using the adequate units we can write the following expression for the Person breathing flow rate

$$b_r = 1.25 \cdot 10^{-4}\ m^3/s \tag{10}$$

The average kind of masks employed are surgical masks, which are estimated to block about $30 - 60\%$ of the particles, leading to a reduction factor $f_a = f_b = 0.4 - 0.7$. In simulations, an average $f_a = f_b = 0.5$ is set, considering a 50% reduction for both the source and inhaled quantities. With all previously explained data we can calculate the inhaled quanta $\mathcal{I}_\phi$. The numerical integration is performed at the end of the simulation as follows:

$$\mathcal{I}_\phi = f_b \cdot \int_0^{t_{end}} \phi(t) \cdot b_r\ dt \tag{11}$$

being $\phi$ $[quanta/m^3]$ the local quanta concentration. Hence, based on the Wells-Riley model we can estimate the probability of infection as:

$$P_i = 1 - e^{-\mathcal{I}_\phi} \tag{12}$$

### 4.2 Risk Matrix

In this work a methodology is defined to evaluate the global risk of contagion with a certain configuration of air sources, e.g. the air conditioning and the air control device. The reference

situation is described as follows: an infected person enters a clean bus an at $t = 0$ min and takes a seat of the ones depicted in Fig. 3a. She/he breathes normally and at $t = 2$ min starts coughing (for about 20 seconds), and then again coughs at $t = 10$ min during 20 s. This person remains in the bus for 20 minutes and then leaves. The contamination effect is tracked within the simulation over 30 minutes. The source profile is shown in Fig. 3b. The probability of contagion is calculated for each person inside the $N$ positions in bus. Then, a new simulation is performed, assuming the infected person takes another seat. This process is repeated for the $N$ seats. The output of this study consists of a risk matrix, corresponding to the risk for a person placed in place $x$ of $N$ (*Susceptible Seats*) of being infected by that person sitting in place $y$ of $N$ (*Infected Seats*). Examples are reported in a graphical way in Fig. 4d. The total sum of the risks provides an overall indication of the risk obtained with a certain configuration. It must be considered that each of these simulations is performed only on the transport of $\phi$ and with a stationary velocity field (which must be resolved only once for each flow field configuration), therefore, the global simulation time is contained.

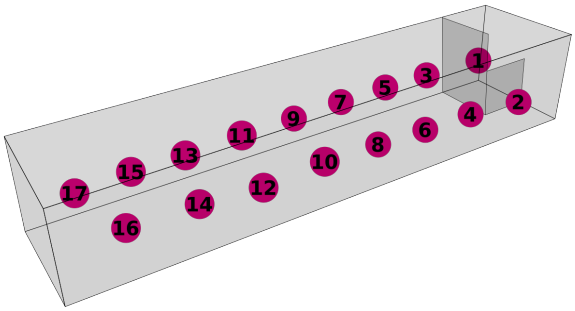


(a) Position of people within the transport vehicle.

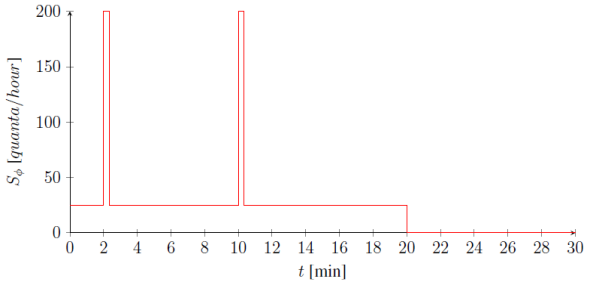


(b) Profile of the exhaled quanta from the infected person

Figure 3: Positions considered for calculating the infection risk, and source profile of the exhaled quanta.

## 5 CONTAMINANT DIFFUSION IN A PUBLIC TRANSPORT VEHICLE

The results obtained on the basic configurations depicted in Fig. 3a are shown and commented in terms of air-age distribution, infection risk, and contaminant distribution. The proposed simulation represents the case of a generic transport vehicle in which the HVAC system is switched on, providing an air flow within the vehicle of 6000 $m^3/h$. The renewal of the internal air, infected by the presence of the virus, is due to the introduction of a percentage of non-recirculated external air (25%). As an example of the possible outputs of the method, some magnitudes of interest were collected along the two lines reported in Fig. 4a. The results regarding air-age are reported in Fig. 4b, where an overall low air-age is observed along the two profiles. The value is particularly low in the center of the domain, while larger values are experienced at the front and back of the bus. The air-age gets specially high in correspondence with the driver seat, although it is not particularly critical as it would correspond to 8 renovations per hour. This is explained by the presence of the glass shield in correspondence behind the

driver's back, which impedes an efficient air renewal. This situation could be resolved by placing inlet air ports around the driver's seat. The concentration of the contaminant PM2.5 would be identical to the outdoor concentration (20 ppm) if no filtration is applied to the outdoor air. The graph in Fig. 4c shows the result of a simulation in which an air filtration device is activated in the front part of the vehicle cabin. It is possible to notice how the concentration is considerably lowered in the areas where the filtration is more effective. The overall risk matrix is reported in Fig. 4d, reporting the infection risk of each susceptible subject to be infected from SARS-CoV-19 by an infected subject placed in each of the positions of the bus. We observe that the seats at the center are the ones that are more prone to causing infection, while the ones at the back, along the ones at the front are the less prone ones. People in the front of the bus, including the driver, are the people with higher probability of contracting infection.

## 6 CONCLUSIONS

A numerical framework aimed at simulating the transport of contaminants and infectious agents within a closed domain is presented in this work. The discussion regarding viruses/contaminants sizes and characteristics serves to identify the model and the diffusive coefficients needed to simulate their behavior within closed environments. Velocity and temperature fields measured on the canonical test case firstly proposed by Nielsen [10] show good agreement with the reference results. The results proposed in the final section, regarding the simulation of a generic transport vehicle, are aimed at providing indications regarding the potentiality of the method.

## ACKNOWLEDGMENT

This work has been developed in the context of the *Rolen Purifica Bus* R&D project, partially financed by INNOTEC (ACCIÓ - Agència per la Competitivitat de l'Empresa, Generalitat de Catalunya). J. Vera has been financially supported by the Ministerio de Educación y Ciencia (MEC), Spain, (FPI grant PRE2018-084017). N. Morozova is supported by the by the Ministerio de Economía y Competitividad, Spain [FPU16/06333 predoctoral contract].

## REFERENCES

[1] N. Morozova, F. X. Trias, R. Capdevila, C. D. Pérez-Segarra and A. Oliva. On the feasibility of affordable high-fidelity CFD simulations for indoor environment design and control. *Building and Environment* (2020) **184**:107144.

[2] Guo, Y., Qian, H., Sun, Z., Cao, J., Liu, F., Luo, X., ... & Zhang, Y. (2021). Assessing and controlling infection risk with Wells-Riley model and spatial flow impact factor (SFIF). Sustainable Cities and Society, 67, 102719.

[3] You, R., Lin, C. H., Wei, D., & Chen, Q. (2019). Evaluating the commercial airliner cabin environment with different air distribution systems. Indoor air, 29(5), 840-853.

[4] Buonanno, G., Morawska, L., & Stabile, L. (2020). Quantitative assessment of the risk of airborne transmission of SARS-CoV-2 infection: prospective and retrospective applications. Environment international, 145, 106112.

[5] B.E. Launder and D.B. Spalding (1974). The numerical computation of turbulent flows. Computer methods in applied mechanics and engineering, 3(2):269–289.

[6] Liu, X., & Zhai, Z. (2007). Identification of appropriate CFD models for simulating aerosol particle and droplet indoor transport. Indoor and Built Environment, 16(4), 322-330.

[7] Hathway, E. A., Noakes, C. J., Sleigh, P. A., & Fletcher, L. A. (2011). CFD simulation of airborne pathogen transport due to human activities. Building and Environment, 46(12), 2500-2511.

[8] Isukapalli, S. S., Mazumdar, S., George, P., Wei, B., Jones, B., & Weisel, C. P. (2013). Computational fluid dynamics modeling of transport and deposition of pesticides in an aircraft cabin. Atmospheric Environment, 68, 198-207.

[9] Lau, Z., Griffiths, I. M., English, A., & Kaouri, K. (2020). Predicting the spatially varying infection risk in indoor spaces using an efficient airborne transmission model. arXiv preprint arXiv:2012.12267.

[10] Nielsen PV, Restivo A, Whitelaw JH (1978). The velocity characteristicsof ventilated rooms. ASME Journal of Fluids Engineering, 100: 291–298.

[11] Limane, A., Fellouah, H., & Galanis, N. (2015, June). Thermo-ventilation study by OpenFOAM of the airflow in a cavity with heated floor. In Building Simulation (Vol. 8, No. 3, pp. 271-283).

[12] Loomans, M., Boerstra, A., & Wisse, C. (2020). Calculating the risk of infection. REHVA Journal , 2020 (5), 19–24.

[13] Nishi, M. (2004). Breathing of humans and its simulation. LSTM-Erlangen Institute of Fluid Mechanic Friedlich-Alexander-University Erlangen.

[14] Wang, Z., Galea, E. R., Grandison, A., Ewer, J., & Jia, F. (2021). Inflight transmission of covid-19 based on experimental aerosol dispersion data. Journal of Travel Medicine, 28 (4).

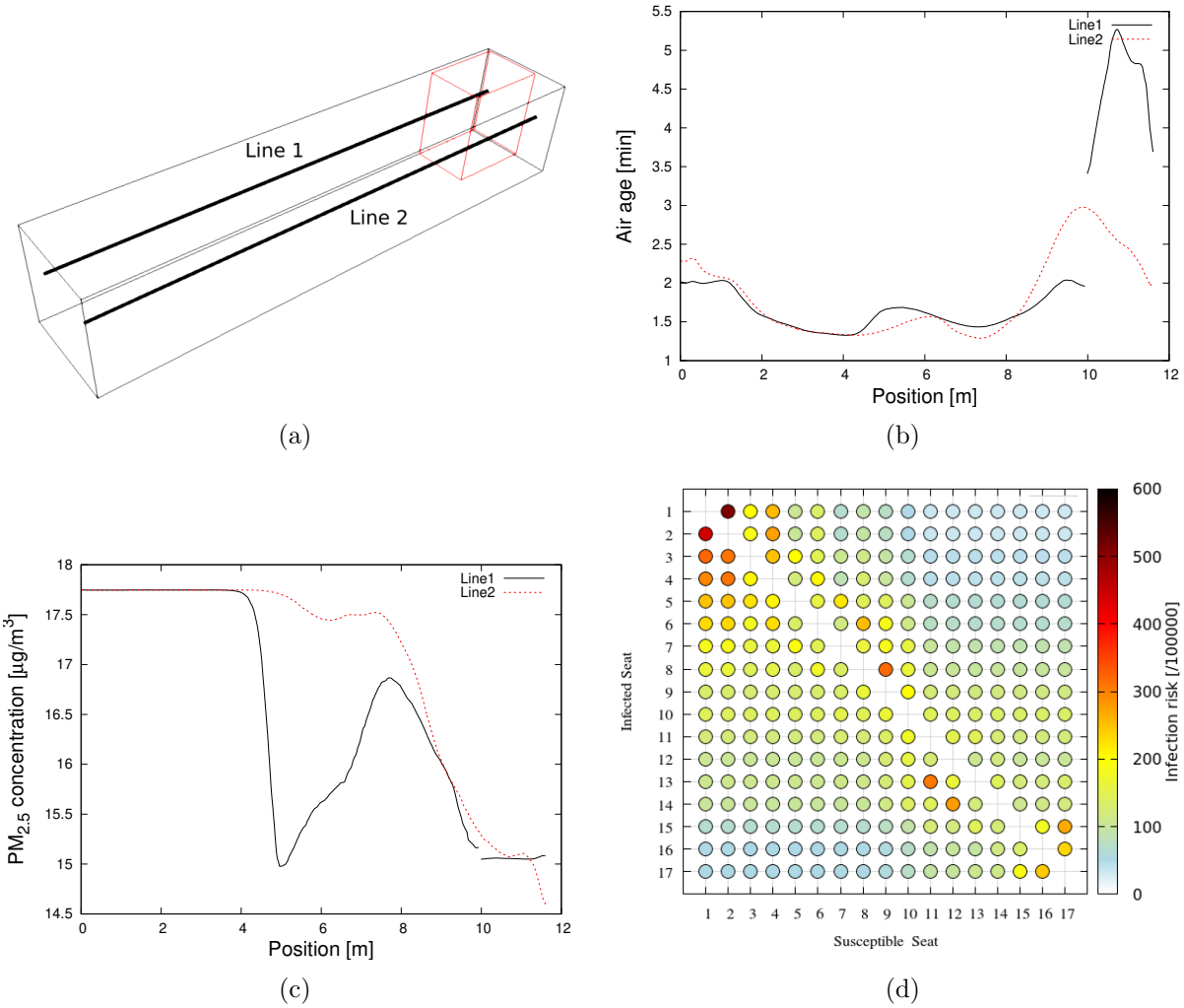


Figure 4: Contaminant transport in a public vehicle: (a) Probing lines; (b) Air-age profiles; (c) PM2.5 concentration inside the bus; (d) Overall risk matrix for SARS-COV-19 Infection.